Available online at www.sciencedirect.com
ScienceDirect
Tetrahedron
Tetrahedron 62 (2006) 12415–12419

Stereodynamics of Ar–CO rotation and conformational preferences of 2-amino-3-(2,4-difluorobenzoyl)-imidazo[1,2-*a*]pyridine

Carlos Jaramillo,[a] José Eugenio de Diego,[a] Alfonso Rivera-Sagredo,[a] Chafiq Hamdouchi[b] and Juan F. Espinosa[a,*]

[a]*Discovery Chemistry Research and Technologies, Lilly Research Laboratories, Centro de Investigación Lilly, Avda de la Industria 30, 28108 Alcobendas, Madrid, Spain*
[b]*Discovery Chemistry Research and Technologies, Lilly Research Laboratories, Lilly Corporate Center, Indianapolis, IN 46285, USA*

Received 4 August 2006; revised 20 September 2006; accepted 27 September 2006
Available online 27 October 2006

Abstract—The dynamic NMR analysis of **2**, a subunit of a new class of cyclic-dependent kinase inhibitors, reveals that the compound exists as two conformational isomers, *Z* and *E*, in acetone, as a consequence of the restricted rotation about the imidazopyridine–carbonyl bond. The less hindered *Z*-rotamer is the most abundant conformer (85:15 *Z*/*E* at 233 K) and the free energy of activation of the interconversion is 13.2 kcal mol^{-1}. The rotamer ratio and the interconversion barrier are similar in other solvents, such as CD_3OD and $CDCl_3$.

1. Introduction

Cyclic-dependent kinases (CDKs) are potential therapeutic targets for the treatment of cancer because they play a key role in initiating and coordinating the phases of the cell-division cycle.[1] In the context of a medicinal chemistry project aimed at the discovery of more efficient and selective CDK inhibitors, we have identified a new family of molecules comprising a 2-aminoimidazo[1,2-*a*]pyridine nucleus bearing benzoyl derivatives on positions 3 and 6.[2] Specifically, we have demonstrated that compounds of type **I** are potent and selective CDK2 inhibitors that compete with ATP for binding to a catalytic unit of the enzyme.[3] CDK2 is one of the most relevant members of the kinase family, since it is involved in two of the four phases of the basic cell-cycle.[4] Imidazopyridines have been shown to have significant potential as new drugs,[5] and they have been exploited to prepare antirhinovirus agents.[6]

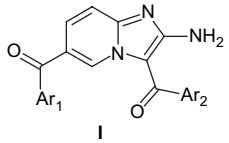

I

In the course of the NMR analysis of **1**, the pronounced broadening of one of the aromatic signals in the ^{1}H spectrum suggested the existence of a slow conformational equilibrium in solution, which was confirmed by the splitting of some signals when the temperature was lowered. Variable-temperature NMR experiments performed for derivatives **2** and **3**, revealed a similar behaviour for **2**, whereas no line-broadening in the temperature range 233–313 K was detected for **3**. This finding indicates that the slow exchange is the result of the benzoyl substitution on position 3 of the imidazopyridine ring.

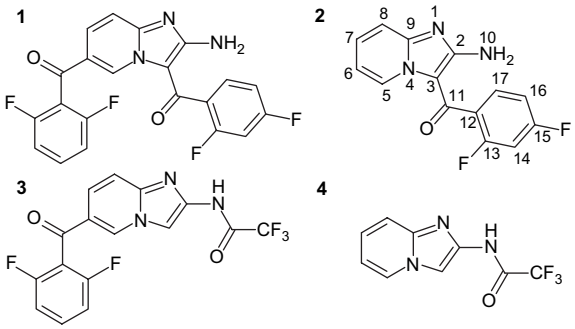

Here, we report on a dynamic NMR study of compound **2** to determine the most abundant conformer in solution, and to measure the value of the rotational barrier involved in the interconversion process. The final goal is to gain a better understanding of the conformational properties of this new

Keywords: Ar–CO rotation; Conformational analysis; Dynamic NMR; Imidazopyridine; CDK inhibitors.
* Corresponding author. Tel.: +34 91 663 3435; fax: +34 91 623 3561; e-mail: jfespinosa@lilly.com

0040–4020/$ - see front matter © 2006 Elsevier Ltd. All rights reserved.
doi:10.1016/j.tet.2006.09.097

class of CDK2 inhibitors to aid the design of more potent derivatives.

2. Results and discussion

The conformational space available to compound **2** was explored by systematic rotation about the C3–C11 and C11–C12 bonds, optimization of the geometry obtained at each incremental step using the MMFF94 force field,[7] and energy calculation. The low-energy conformations were subjected to an energy minimization by the semi-empirical AM1 method[8] to obtain more refined structures. According to the AM1 calculations, the C3–C11–C12–C13 dihedral angle is close to 90°, similar to that of *ortho*-substituted diaryl or alkyl aryl ketones that adopt twisted conformations (dihedral angle in the range 60°–90°),[9] whereas the C2–C3–C11–CO dihedral angle is close to 0°, as described for benzaldehydes, even when *ortho*-substituted (Fig. 1).[9] As a consequence, rotation about C11–C12 interconverts two conformational enantiomers; the process is NMR-invisible, given the absence of substituents that can serve as prochiral probes. Conversely, rotation about C3–C11 interconverts two conformational isomers, *Z* and *E* (Fig. 1), and, provided that the rate of rotation is rendered sufficiently slow on the NMR time-scale, separated signals corresponding to each rotamer will be observed. Therefore, the conformational equilibrium detected for **2** must originate from slow rotation about the sp^2–sp^2 C3–C11 bond.

The ^{1}H spectrum of **2** in acetone at 303 K showed seven aromatic signals (Fig. 2a), three of them corresponding to the difluorobenzoyl protons, easily identified through the coupling to the ^{19}F nuclei, and the other four corresponding to the imidazopyridine protons: a doublet at 7.35 ppm, a triplet at 7.55 ppm, a broad triplet at 6.99 ppm and a very broad peak at 9.25 ppm. The broadening of the latter two signals was attributed to the proximity of the protons to the slow-rotating Ar–CO, and the signals assigned to H6 and H5, respectively. This assignment was confirmed through HMBC and COSY experiments (see Supplementary data). While the triplet at 7.55 ppm showed a long-range H,C correlation to a non-protonated carbon at 149.0 ppm (C9) in an HMBC experiment, such correlation was not detected for the triplet at 6.99 ppm, indicating that the former triplet corresponded to H7, three bonds away from C9, and the latter to H6. A coupling between H7 and H8, observed in a COSY experiment, led to the assignment of the doublet at 7.35 ppm to H8.

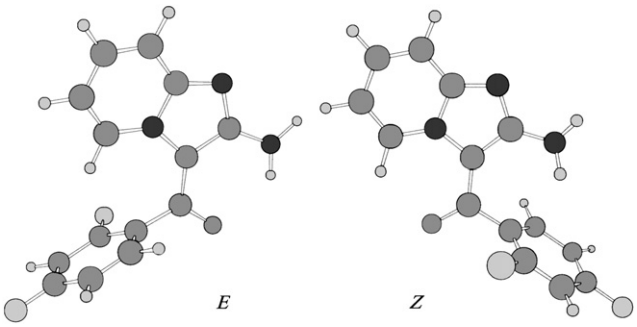

Figure 1. AM1-computed structures of the *E* and *Z* conformers of **2**.

The ^{1}H spectrum at 233 K showed two sets of signals in an 85:15 ratio; however, because of severe resonance overlapping, not all the minor peaks were identified (Fig. 2b). In particular, H5 major appeared at 9.69 ppm in a clean region of the spectrum; however, the position of the corresponding proton signal for the minor rotamer was unclear. The signal of H5 minor was detected through the selective inversion of H5 major in a 1D nuclear Overhauser effect spectroscopy (NOESY) experiment at 233 K, which gave rise to an exchange peak at 7.58 ppm (Fig. 2c). Two additional signals of opposite sign were present in the 1D NOESY spectrum, corresponding to NOEs between H5 and H6 for both rotamers. This result indicates that the rotamers, which are in slow exchange on the chemical shift time-scale, are in fast exchange on the T_1 time-scale.

The large chemical shift difference between H5 protons can be related to the conformational arrangement about the C3–C11 bond, allowing the assignment of the conformational isomers. H5 major is shifted to a higher frequency by 1.10 ppm, and H5 minor is shifted to a lower frequency by 1.01 ppm, with respect to the same proton in reference compound **4**. Because in the *Z*-rotamer H5 is in close proximity to the carbonylic oxygen atom (Fig. 1), the major species can be assigned to the *Z*-rotamer, where the deshielding experienced by H5 can be interpreted as a consequence of the through-space effect of the oxygen atom. Hence, the minor species would correspond to the *E*-rotamer, where H5 is shielded by the anisotropic effect of the benzoyl aromatic ring (Fig. 1). Consistently, the opposite trend was found for the NH_2 protons, which are shielded in the major rotamer by 1.54 ppm relative to the minor rotamer. The AM1 results suggest that the most abundant *Z*-rotamer is slightly more stable than the *E*-rotamer, by 0.14 kcal mol^{-1}.

Because the minor *E*-rotamer places the carbonylic oxygen atom within hydrogen bonding distance of the amine protons, the occurrence of intramolecular hydrogen bonding between these atoms can be envisaged. If this were the case, the population of this rotamer would be expected to show some dependence on the polarity of the solvent. This hypothesis was investigated by recording ^{1}H spectra of **2** in other solvents within the solubility limits of the compound ($CDCl_3$ and CD_3OD). The spectra also showed splitting of signals at 233 K, and the rotamer ratios were fairly similar to those in acetone (Table 1), demonstrating that the change of solvent polarity does not modify the conformational preferences. Thus, the existence of a hydrogen bond between the carbonylic oxygen atom and the amino protons cannot be inferred from NMR data.

Full line shape analysis of the ^{1}H spectra as a function of temperature led to the rate constants of the interconversion and to the barrier for rotation about the C3–C11 bond. The free-energy barrier of interconversion of the more stable into the less stable form in acetone is 13.2 kcal mol^{-1}. Similar line shape analysis was performed in $CDCl_3$ and CD_3OD, and yielded similar values (Table 1), indicating little influence of the solvent in the rate of interconversion, as those for the rotamer ratios.

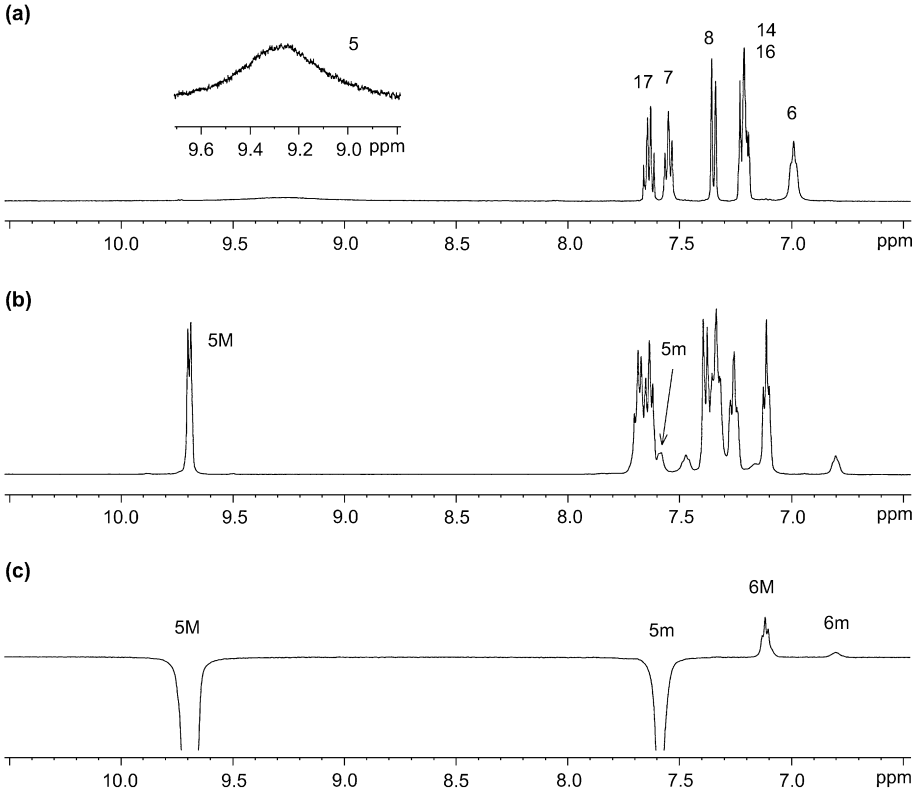

Figure 2. The 500 MHz spectra of **2** in acetone-d_6. (a) ^{1}H at 303 K; (b) ^{1}H at 233 K; (c) 1D NOESY at 233 K. The assignment of the resonances is shown. M, major; m, minor.

Rotation about the bond between an aromatic ring and a carbonyl group has been thoroughly studied by dynamic NMR spectroscopy. Interestingly, the energy barrier of the Ar–CO rotation measured in **2** is similar to those reported for some aromatic ketones bearing bulky substituents on *ortho*-positions such as **5** and **6** (Table 2).[10,11]

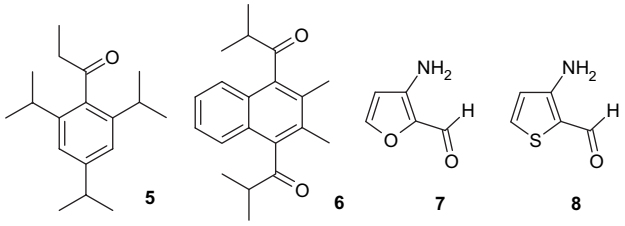

However, the root cause of the barrier to internal rotation differs in both types of structures. While the *ortho*-disubstituted ketones have the carbonyl group arranged essentially orthogonal to the aromatic ring and the rotation barrier is of a steric nature, the carbonyl group and the imidazopyridine are almost coplanar in **2**, and the barrier to rotation about the C3–C11 bond (π-barrier) originates from the stabilization of the carbonyl group brought about by the mesomeric effect of the aminoimidazopyridine ring (Scheme 1). In this respect, the energy barriers would be better compared with those measured in five-membered heteroaromatic *o*-aminoaldehydes such as **7** and **8**, which present the same type of conjugation (Table 2).[12] Interestingly, the value for the Ar–CO rotation in **2** is similar to that of **8**, indicating a similar degree of conjugation between the aromatic ring and the carbonyl group in the 2-aminoimidazopyridine and in the 3-aminothiophene.

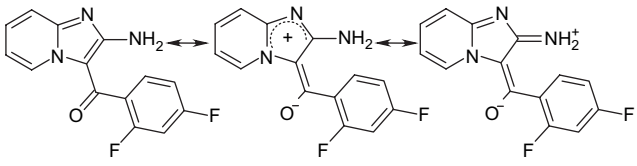

Scheme 1.

Table 1. Interconversion barrier ($\Delta G^{\ddagger}$), conformer ratio at 233 K and chemical shift difference (Δd) of the monitored resonance (H6) at 233 K for **2**

Solvent	$\Delta G^{\ddagger}$ (kcal mol^{-1})	*Z*/*E* ratio	Δd (Hz, 500 MHz)
Acetone-d_6	13.2	85:15	154.4
$CDCl_3$	13.4	81:19	173.1
CD_3OD	13.0	82:18	165.5

Table 2. Free energies of activation ($\Delta G^{\ddagger}$) for Ar–CO rotation in several aromatic compounds

Compound	$\Delta G^{\ddagger}$ (kcal mol^{-1})	Solvent
2	13.2	Acetone-d_6
5	13.5	CD_2Cl_2
6	13.4	CD_2Cl_2
7	16.2	DMSO-d_6
8	13.7	CD_3CN

3. Conclusions

Variable-temperature NMR analysis of **2** demonstrates the coexistence of two conformational isomers in solution undergoing interconversion about the imidazopyridine–CO bond. In both rotamers, the carbonyl bond is coplanar to the imidazopyridine ring and orthogonal to the difluorobenzoyl ring. The *Z*-rotamer is the predominant conformation in solution, and the rotamer ratio is little affected by solvent changes. This finding indicates that the conformational preferences of **2** are intrinsic and not driven by interactions with the solvent molecules. Although the barriers to rotation about Ar–CO bonds have received considerable attention, to the best of our knowledge, this is the first time that the stereodynamics of the Ar–CO bond has been measured for an imidazopyridine ring, which is an important class of heterocyclic compounds. The results of further studies investigating the influence of the structure of the benzoyl ring on the rotamer ratio and on the rate of interconversion will be reported in due course.

4. Experimental

4.1. Materials

The title compound (**2**) was prepared following the general procedure described in Refs. 2 and 13. The assignment of the proton resonances is discussed in the text. ^{1}H NMR (500 MHz, acetone-d_6 at 30 °C): δ=9.25 (br s, 1H, H5), 7.63 (q, J=7.5 Hz, 1H, H17), 7.55 (t, J=7.6 Hz, 1H, H7), 7.35 (d, J=8.5 Hz, 1H, H8), 7.21 (m, 2H, H14 and H16), 6.99 (br t, 1H, H6), 5.39 (br s, 2H, NH_2). ^{13}C NMR (75 MHz, acetone-d_6 at 30 °C): δ=176.4 (C11), 164.9 (dd, J=250.3 Hz, 11.8 Hz, C15), 160.3 (dd, J=250.6 Hz, 12.6 Hz, C13), 160.1 (C2), 149.0 (C9), 131.7 (C7), 131.5 (dd, J=10.1 Hz, 5.2 Hz, C17), 129.3 (br s, C5), 126.4 (dd, J=17.5 Hz, 4.0 Hz, C12), 115.1 (C6), 113.7 (C8), 113.5 (dd, J=21.5 Hz, 3.7 Hz, C16), 109.3 (C3), 105.9 (t, J=25.9 Hz, C14). MS (EI): m/z 274 $[M+H]^+$.

4.2. NMR spectroscopy

The variable-temperature NMR spectra were acquired on a Bruker DRX 500 Avance spectrometer equipped with a 5-mm inverse probe. Proton and carbon chemical shifts were referenced to the residual solvent signals. Temperature calibration on the spectrometer was performed using a standard methanol sample. Proton spectra were acquired using 32K data points and zero-filled to 64K. The 1D NOESY experiments were carried out with the selective 1D double-pulse field gradient spin echo module[14] using a mixing time of 500 ms. Absolute value correlated spectroscopy (COSY), phase-sensitive heteronuclear single quantum coherence (HSQC) and heteronuclear multiple-bond correlation (HMBC) data were acquired using gradient selection techniques. Acquisition data matrices were defined by 1K×256 points in F_2 and F_1, respectively. The 2D data matrices were multiplied by the appropriate window functions and zero-filled to 2K×1K matrices. Linear prediction was applied before Fourier transformation, and polynomial baseline correction was used in both dimensions of the 2D spectra. Data were processed using the XWINNMR Bruker program on a Silicon Graphics computer. The energy barriers were determined by full line shape analysis of H6 resonance at various temperatures within the 223–313 K range (see Supplementary data). The corresponding free energies of activation were independent of temperature within the errors (±0.3 kcal mol^{-1}) and the average value was taken as the interconversion barrier. Similar values were obtained through line shape analysis of H5 resonance. The simulation was performed using a line-fitting program based on the Bloch equations in the presence of chemical exchange, and the best fit was judged visually by superimposing the predicted and experimental spectra.

Supplementary data

Supplementary data associated with this article can be found in the online version, at doi:10.1016/j.tet.2006.09.097.

References and notes

1. (a) Sherr, C. J. *Science* **1996**, *274*, 1672; (b) Hunter, T. *Cell* **1997**, *88*, 333; (c) Pavletich, N. P. *J. Mol. Biol.* **1999**, *287*, 821; (d) Malumbres, M.; Barbacid, M. *Nat. Rev. Cancer* **2001**, *1*, 222.
2. (a) Jaramillo, C.; de Diego, J. E.; Hamdouchi, C.; Collins, E.; Keyser, H.; Sanchez-Martínez, C.; del Prado, M.; Norman, B.; Brooks, H. B.; Watkins, S. A.; Spencer, C. D.; Dempsey, J. A.; Anderson, B. D.; Campbell, R. M.; Legget, T.; Patel, B.; Schultz, R. M.; Espinosa, J.; Vieth, M.; Zhang, F.; Timm, D. E. *Bioorg. Med. Chem. Lett.* **2004**, *14*, 6095; (b) Hamdouchi, C.; Zhong, B.; Mendoza, J.; Collins, E.; Jaramillo, C.; de Diego, J. E.; Robertson, D.; Spencer, C. D.; Anderson, B. D.; Watkins, S. A.; Zhang, F.; Brooks, H. B. *Bioorg. Med. Chem. Lett.* **2005**, *15*, 1943.
3. Hamdouchi, C.; Keyser, H.; Collins, E.; Jaramillo, C.; de Diego, J. E.; Spencer, C. D.; Dempsey, J. A.; Anderson, B. D.; Leggett, T.; Stamm, N. B.; Schultz, R. M.; Watkins, S. A.; Cocke, K.; Lemke, S.; Burke, T. F.; Beckmann, R. P.; Dixon, J. T.; Gurganus, T. M.; Rankl, N. B.; Houck, K. A.; Zhang, F.; Vieth, M.; Espinosa, J.; Timm, D. E.; Campbell, R. M.; Patel, B. K. R.; Brooks, H. B. *Mol. Cancer Ther.* **2004**, *3*, 1.
4. Sorensen, C. S.; Lukas, C.; Kramer, E. R.; Peters, J.-M.; Bartek, J.; Lukas, J. *Mol. Cell. Biol.* **2001**, *21*, 3692.
5. (a) Kaminski, J. J.; Puchalski, C.; Solomon, D. M.; Rizvi, R. K.; Conn, D. J.; Elliot, A. J.; Lovey, R. G.; Guzik, H.; Chiu, P. J. S.; Long, J. F.; McPhail, A. T. *J. Med. Chem.* **1989**, *32*, 1686; (b) Bonnet, P. A.; Michel, A.; Laurent, F.; Sablayrolles, C.; Rechencq, E.; Mani, J. C.; Boucard, M.; Chapat, J. P. *J. Med. Chem.* **1992**, *35*, 3353.
6. Hamdouchi, C.; Ezquerra, J.; Vega, J. A.; Alvarez-Builla, J.; Heinz, B. A. *Bioorg. Med. Chem. Lett.* **1999**, *9*, 1391.
7. Halgren, T. A. *J. Comput. Chem.* **1996**, *17*, 490.
8. Dewar, M. J. S.; Zoebisch, E. G.; Healy, E. F.; Stewart, J. J. P. *J. Am. Chem. Soc.* **1985**, *107*, 3902.
9. (a) Abraham, R. J.; Angiolini, S.; Edgar, M.; Sancassan, F. *J. Chem. Soc., Perkin Trans. 2* **1995**, 1973; (b) Abraham, R. J.; Angiolini, S.; Edgar, M.; Sancassan, F. *J. Chem. Soc., Perkin Trans. 2* **1997**, 41.

10. Casarini, D.; Lunazzi, L.; Verbeek, R. *Tetrahedron* **1996**, *52*, 2471.
11. Casarini, D.; Lunazzi, L.; Mazzanti, A. *J. Org. Chem.* **1998**, *63*, 4991.
12. Lunazzi, L.; Mazzanti, A.; Spagnolo, P.; Degl'Innocenti, A. *J. Org. Chem.* **1997**, *62*, 2263.
13. Jaramillo, C.; Carretero, J. C.; de Diego, J. E.; del Prado, M.; Hamdouchi, C.; Roldán, J. L.; Sánchez-Martínez, C. *Tetrahedron Lett.* **2002**, *43*, 9051.
14. Stott, K.; Stonehouse, J.; Keeler, J.; Hwang, T.-L.; Shaka, A. J. *J. Am. Chem. Soc.* **1995**, *117*, 4199.